

FILE COPY

2

AD-A222 539



**DEPARTURES FROM PLANE-WAVE-LIKE  
COUPLING TO A MAVERICK MISSILE  
IN THE RADIATING NEAR-FIELD  
REGION OF A HORN ANTENNA**

D. E. Voss, et al

Voss Scientific  
Albuquerque, NM 87108

May 1990

Final Report

DTIC  
ELECTE  
JUN 08 1990  
S D D

Approved for public release; distribution unlimited.

**Weapons Laboratory  
Air Force Systems Command  
Kirtland Air Force Base, NM 87117-6008**

This final report was prepared by Voss Scientific, Albuquerque, New Mexico, under Contract F29601-86-C-0212, Job Order 57970198, with the Weapons Laboratory, Kirtland Air Force Base, New Mexico. Captain Lynn M. Miner (AWK) was the Laboratory Project Officer-in-charge.


When Government drawings, specifications, or other data are used for any purpose other than in connection with a definitely Government-related procurement, the United States Government incurs no responsibility or any obligation whatsoever. The fact that the Government may have formulated or in any way supplied the said drawings, specifications, or other data, is not to be regarded by implication, or otherwise in any manner construed, as licensing the holder, or any other person or corporation; or as conveying any rights or permission to manufacture, use, or sell any patented invention that may in any way be related thereto.

This report has been authored by employees and a contractor of the United States Government. Accordingly, the United States Government retains a non-exclusive, royalty-free license to publish or reproduce the material contained herein, or allow others to do so, for the United States Government purposes.

This report has been reviewed by the Public Affairs Office and is releasable to the National Technical Information Service (NTIS). At NTIS, it will be available to the general public, including foreign nationals.


If your address has changed, if you wish to be removed from our mailing list, or if your organization no longer employs the addressee, please notify WL/AWK, Kirtland AFB, NM 87117-6008 to help us maintain a current mailing list.

This technical report has been reviewed and is approved for publication.



LYNN M. MINER  
Captain, USAF  
Project Officer

FOR THE COMMANDER



JAMES W. O'CONNOR  
Major, USAF  
Chief, HPM Simulators Division

DO NOT RETURN COPIES OF THIS REPORT UNLESS CONTRACTUAL OBLIGATIONS OR NOTICE ON A SPECIFIC DOCUMENT REQUIRES THAT IT BE RETURNED.

REPORT DOCUMENTATION PAGE			Form Approved OMB No. 0704-0188	
Public reporting burden for this collection of information is estimated to average 1 hour per response, including the time for reviewing instructions, searching existing data sources, gathering and maintaining the data needed, and completing and reviewing the collection of information. Send comments regarding this burden estimate or any other aspect of this collection of information, including suggestions for reducing this burden, to Washington Headquarters Services, Directorate for Information Operations and Reports, 1215 Jefferson Davis Highway, Suite 1204, Arlington, VA 22202-4302, and to the Office of Management and Budget, Paperwork Reduction Project (0704-0188), Washington, DC 20503.				
1. AGENCY USE ONLY (Leave blank)	2. REPORT DATE May 1990	3. REPORT TYPE AND DATES COVERED Final Mar 89 - Dec 89		
4. TITLE AND SUBTITLE DEPARTURES FROM PLANE-WAVE-LIKE COUPLING TO A MAVERICK MISSILE IN THE RADIATING NEAR-FIELD OF A HORN ANTENNA		5. FUNDING NUMBERS C: F29601-86-C-0212 PE: 62601F PR: 5797 TA: 01 WU: 98		
6. AUTHOR(S) Voss, D. E. Cremer, C. D. Minér, L. M. Koslover, R. A. Silvestro, J.				
7. PERFORMING ORGANIZATION NAME(S) AND ADDRESS(ES) Voss Scientific Albuquerque, NM 87108		8. PERFORMING ORGANIZATION REPORT NUMBER		
9. SPONSORING/MONITORING AGENCY NAME(S) AND ADDRESS(ES) Weapons Laboratory Kirtland AFB, NM 87117-6008		10. SPONSORING/MONITORING AGENCY REPORT NUMBER  WL-TR-90-04		
11. SUPPLEMENTARY NOTES  <i>Cambridge</i>				
12a. DISTRIBUTION/AVAILABILITY STATEMENT  Approved for public release; distribution unlimited.  L		12b. DISTRIBUTION CODE  <i>Approved</i>		
13. ABSTRACT (Maximum 200 words) The HPM susceptibility testing often requires irradiating test objects at the highest fluences possible. For aperture antennas, the highest fluences are generally found in the radiating near-field region. For valid effects testing, the energy coupled to the object interior must accurately replicate that which would occur in a true weapon environment (plane-wave illumination). Some believe that valid testing requires object placement at distances from the aperture exceeding $2D^2/\lambda$ (D=antenna effective diameter). Many also believe testing at farther away than $2D^2/\lambda$ guarantees plane-wave-like coupling conditions. Neither view is correct. Testing in the reactive field region ( $<\lambda$ from the aperture) is generally invalid due to dominance of reactive coupling. For testing in the radiating near field, determination of validity is less trivial. An investigation was performed quantifying deviations from plane-wave coupling in the radiating near field, for head-on illumination of a Maverick missile in the 1-4 GHz range. The measurements, using an instrumented Maverick missile in an anechoic chamber, and supported by theory, indicate conditions for which testing the Maverick missile accurately simulates plane-wave coupling.  <i>RH</i>				
14. SUBJECT TERMS Near-field High Power Microwave Susceptibility Testing Energy Fluence Antennas			15. NUMBER OF PAGES 26	
			16. PRICE CODE	
17. SECURITY CLASSIFICATION OF REPORT Unclassified	18. SECURITY CLASSIFICATION OF THIS PAGE Unclassified	19. SECURITY CLASSIFICATION OF ABSTRACT Unclassified	20. LIMITATION OF ABSTRACT	

## SUMMARY

It is often desirable to irradiate test objects at the highest fluences possible to verify hardness as well as determine potential susceptibility to future high power microwave (HPM) threats. When using aperture antennas, such as conical or pyramidal horns, the highest fluences are generally found in the radiating near-field region. However, for effects testing to be valid, the energy coupled to the interior of the object must accurately replicate that which would occur in a true weapon environment, i.e., plane-wave illumination. Some in the HPM community mistakenly believe that testing can be valid only for placement of test objects at distances farther from the aperture than  $2 D^2/\lambda$ , where D is equal to the effective diameter of the aperture antenna. Many also believe testing at distances farther from the source than  $2 D^2/\lambda$  guarantees plane-wave-like coupling conditions. Neither view is correct. Testing in the reactive near-field region (confined to  $<1-2 \lambda$  from the aperture) is generally invalid due to reactive coupling being dominant. However, for testing performed in the radiating near field, the determination of validity is less straightforward.

A systematic experimental investigation has been performed to quantify the deviations relative to plane-wave coupling occurring in the radiating near field for the case of head-on illumination of a Maverick missile at frequencies in the 1-4 GHz range. The measurements, utilizing an instrumented Maverick missile in an anechoic chamber and supported by theoretical models, indicate the condition for which testing the Maverick missile in the radiating near field accurately simulates plane-wave coupling. This condition is as follows:

If the beam cross-sectional area exceeds the projected geometrical cross-sectional area of the missile by a factor of 2 or more, then the energy coupled to the interior will deviate by no more than 1 dB from that which would occur under uniform plane-wave illumination at the same spatially averaged power and fluence.

Beam cross-sectional area is defined as corresponding to the 3 dB points in the E and H planes.



111/iv

DTIC	
COPY INSPECTED 6	
Availability Codes	
Dist	Avail and/or Special
A-1	

## INTRODUCTION

It is often desirable to irradiate test objects at the highest fluences and highest powers possible, both from the point of view of verifying hardness as well as determining potential susceptibility to any future high power microwave (HPM) threat. The highest fluence available from an aperture antenna, such as a conical or pyramidal horn, is generally found at a short distance from the aperture, generally in the radiating near-field region (Ref. 1). The key issue that must be addressed when testing in the radiating near field is whether the microwave coupling conditions are effectively equivalent to those that would exist for incident plane-wave illumination from a distant source. It is essential to recognize that the question "Do we have plane-wave-like coupling conditions?" is not equivalent to the question "Is the test object in the far-field region?" Plane-wave-like coupling conditions can often exist at distances substantially closer to the aperture than  $2 D^2/\lambda$ . Alternatively, in some circumstances, plane-wave-like coupling conditions may not exist even at distances substantially  $>2 D^2/\lambda$ . When the former is the case, it is possible to test systems at power and fluences which significantly exceed ( $\sim 10$  dB) levels available at  $2 D^2/\lambda$ . Ultimately, the determination of whether plane-wave-like coupling conditions exist must be made by careful consideration of effects depending on the geometry of both the antenna and the test object, as well as the wavelength of the radiation.

Experimental and theoretical work has been performed to quantify the significance of effects that could lead to other than plane-wave-like coupling conditions for placement of the Maverick missile in the radiating near-field regions of horn antennas. Departures from plane-wave-like coupling due to the following effects were considered:

- Illumination with a nonuniform power density.
- Standing waves generated by reflections between the missile and the horn.
- Reactive coupling of power from the horn to the missile.

This report describes a set of experiments which led to intuitive criteria for validity of plane-wave coupling. Additionally, an important tool for

interpretation of the data, an aperture antenna code validated to an accuracy of better than  $\pm 0.3$  dB for the radiating near-field region, is described in the Appendix.

## REGIONS ABOUT AN APERTURE ANTENNA

It is important to clarify the terms used to differentiate the various regions relative to a radiating source. The term radiating near field refers to a region of space surrounding an antenna that is between the reactive near-field region and the far-field region. The reactive near field is the region of space where reactive (i.e., capacitive and inductive) effects dominate. Reactive field amplitudes fall off very rapidly with increasing distance and become negligible within a few wavelengths from the source. Next is the radiating near-field region in which, by definition, the angular distribution of the radiated fields is a function of the separation between the source and the measurement locations. Finally, the far-field region begins at distances sufficiently far from the source that the angular distribution of the radiating fields is independent of the source to measurement separation. For aperture antennas, these three regions of space are specified by the following approximate criteria (Ref. 2):

$$r \leq \lambda \quad \text{reactive near-field region}$$

$$\lambda \leq r \leq 2 D^2/\lambda \quad \text{radiating near-field region}$$

$$r \geq 2 D^2/\lambda \quad \text{far-field region}$$

where  $D$  is the effective aperture diameter.

## COLD-TESTING IN ANECHOIC CHAMBER

### EXPERIMENTAL APPROACH

Separate tests were performed using two continuous wave-driven externally-leveled  $TE_{10}$ -mode pyramidal horns for L-band (1.12-1.70 GHz) and S-band (2.60-3.95 GHz). Tests were carried out in a 40 x 20 x 20 ft anechoic chamber in which the conducting walls are lined with a 2-ft-tall pyramidal-type microwave absorber. For the frequencies and geometry used here, relevant wall

reflections are reduced by at least 45 dB compared to the incident wave in all cases. Because of considerable similarity of  $TE_{10}$ -driven pyramidal horn patterns to  $TE_{11}$ -driven conical horn patterns, the experimental results are also relevant to testing with conical horns operated in fundamental mode. The experiments described will thus be used to validate HPM testing of Maverick using the Weapons Laboratory's (WL) Double Anode Relativistic Tetrode (DART) source, which utilizes the recently developed finned asymmetric cone  $TM_{01}$  to  $TE_{11}$  mode converter (Ref. 3) to radiate a pencil beam from a conical horn in  $TE_{11}$  mode.

The experiment consisted of exposing an instrumented AGM-65D Maverick missile guidance and control section to head-on illumination in the radiating near- and far-field regions of pyramidal horns (Fig. 1). Signals from various probes in the seeker and electronics sections were simultaneously monitored as frequency was scanned across L-band and S-band. Frequencies between these bands, 1.70-2.60 GHz, were not tested because of unavoidable time limitations. In each case, far-field values of effective areas for three of the several in situ missile probes/sensors\* were obtained by placing the Maverick missile seeker head in the far field of the radiating horn at on-axis radial positions  $r \gg 2D^2/\lambda$ . The effective area of each in situ probe was defined as the ratio of the power collected by the probe to the computed unperturbed incident power density averaged over the missile window. The power density was computed using the validated code described in detail in the Appendix to an estimated accuracy of  $\pm 0.2$  dB. The reflected power coupled back into the radiating horn was also recorded to determine the significance of possible standing wave formation between the horn and missile.

Effective areas were measured for individual sensors at each axial location at each of several observed peaks in the coupling transfer function in each frequency band. Thus, any perturbations to the distribution of power density at the window that influence coupling, due to any or all of the effects mentioned previously, appear as changes in probe effective areas as the missile is varied in axial location. To avoid confusion caused by a possible nonlinear relationship between power measured at the missile sensors and the unperturbed incident power density at the window (an effect unrelated to considerations

\*Supplied and installed by R. Achenbach and R. Bonn of JAYCOR.

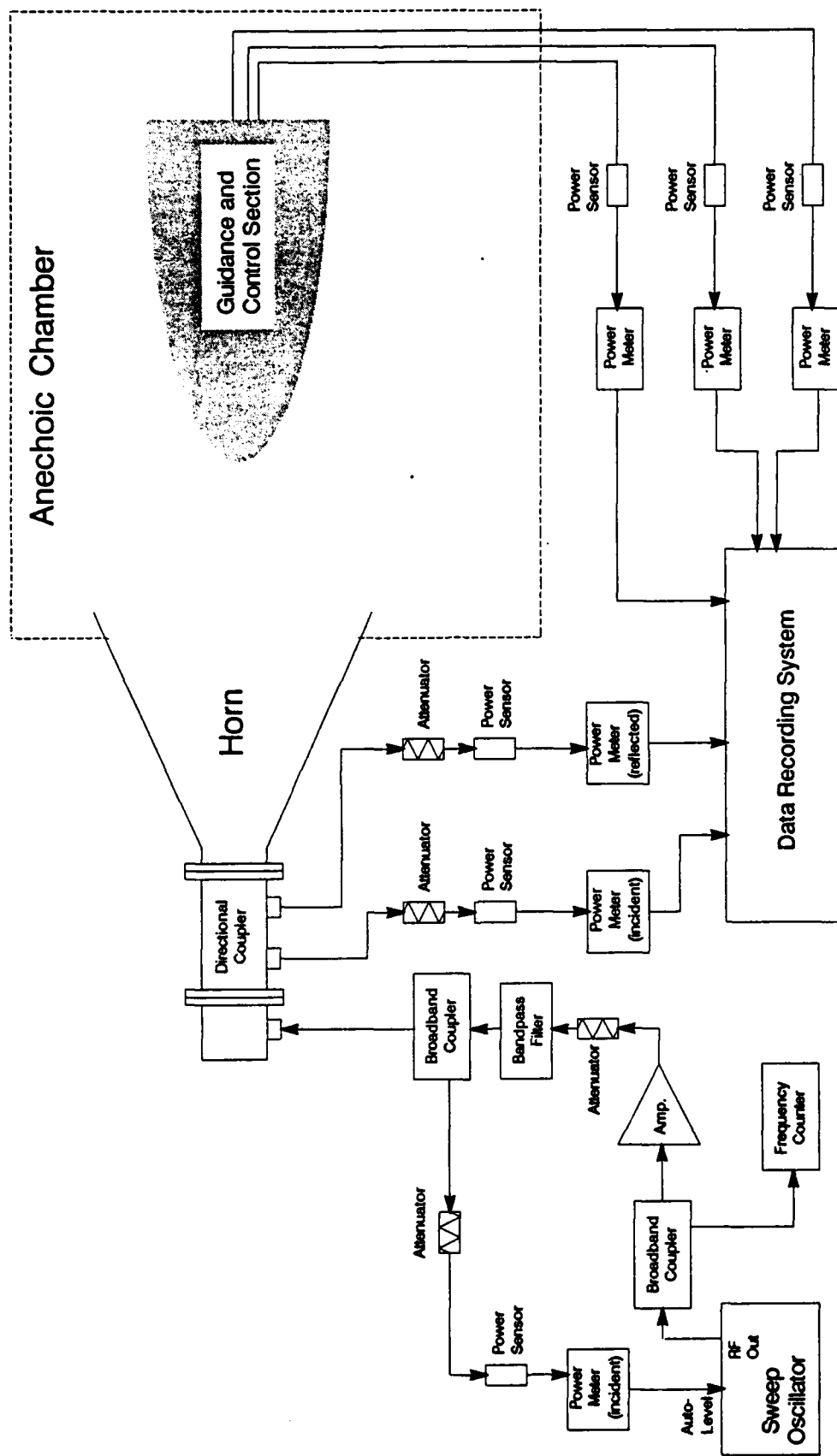


Figure 1. Schematic of the experimental apparatus.

incident power density at the window (an effect unrelated to considerations of the validity of radiating near-field testing), we adjusted the total horn output power so that the unperturbed power density averaged over the missile infrared (IR) window was kept nearly constant as the missile was varied in axial position. Thus, the differences in coupling observed as the missile was moved axially should be attributable to departures from plane-wave-like coupling conditions. There is some measurable scatter in the data, even at various far-field locations, which is attributed to small uncontrollable misalignments of the missile due to irreproducible rotations and tilts resulting from the repositioning of the missile at each axial location. Nevertheless, the signal-to-noise ratio is sufficiently large to observe any consistent departures from plane-wave-like coupling conditions that exceed 0.5 dB.

### RESULTS AND ANALYSES

Departure from plane-wave-like coupling conditions was found to occur only in combination with comparably nonuniform illumination. For all of the in situ probes used for these experiments, any difference between their effective areas measured in the radiating near field and those measured in the far field exceeding  $\pm 1.5$  dB only occurred when the nonuniformity of illumination over the missile window also exceeded  $\pm 1.5$  dB. Reduced data for each of the three probe signals at both L- and S-bands are shown in Figure 2. Each of the six curves represents an average of the absolute deviation from far-field effective area  $A_{\text{eff}}$  for several frequency peaks in each band. The combined L- and S-band data from Figure 2 can be averaged to produce the overall summary of the experimental data shown in Figure 3.

Note that the abscissa in Figures 2 and 3 is labeled  $A_{\text{beam}}/A_{\text{missile}}$  rather than the aperture-to-missile separation distance. This representation is more useful than a plot versus axial distance since  $A_{\text{beam}}$  has a substantial frequency dependence. By plotting the data as shown, this frequency dependence to the beam width is effectively removed, and the L- and S-band data become generally consistent.  $A_{\text{beam}}$  is defined as the area of the beam (in a flat x-y plane) such that the power density at the edge of the beam in the E and H planes falls off to half of the on-axis value. This quantity was calculated for each axial position and at each frequency using the validated code described in the Appendix. Typical data for conversion from axial position to

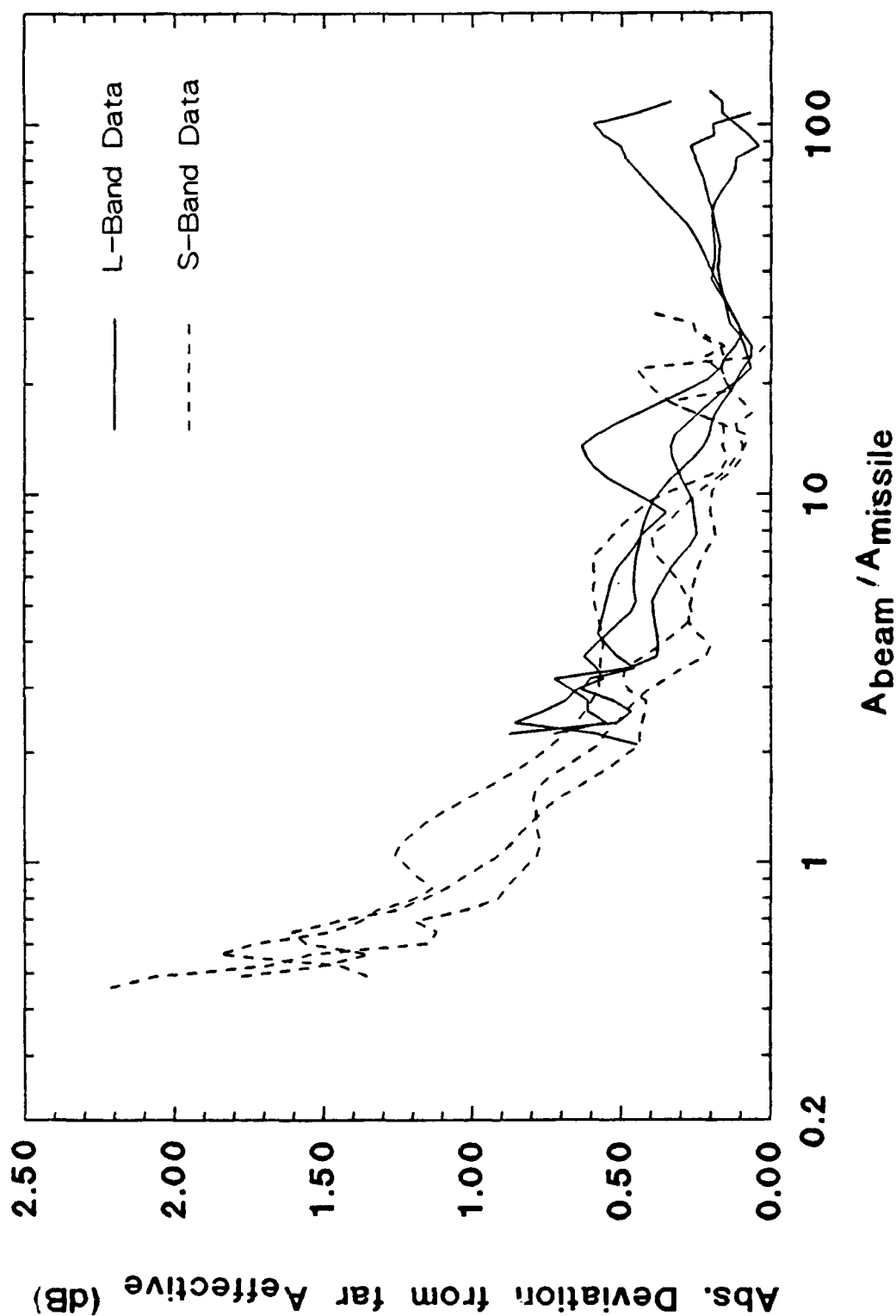


Figure 2. Change in  $A_{eff}$  from its far-field value for three sensors monitored at L- and S-bands, as axial distance is varied.

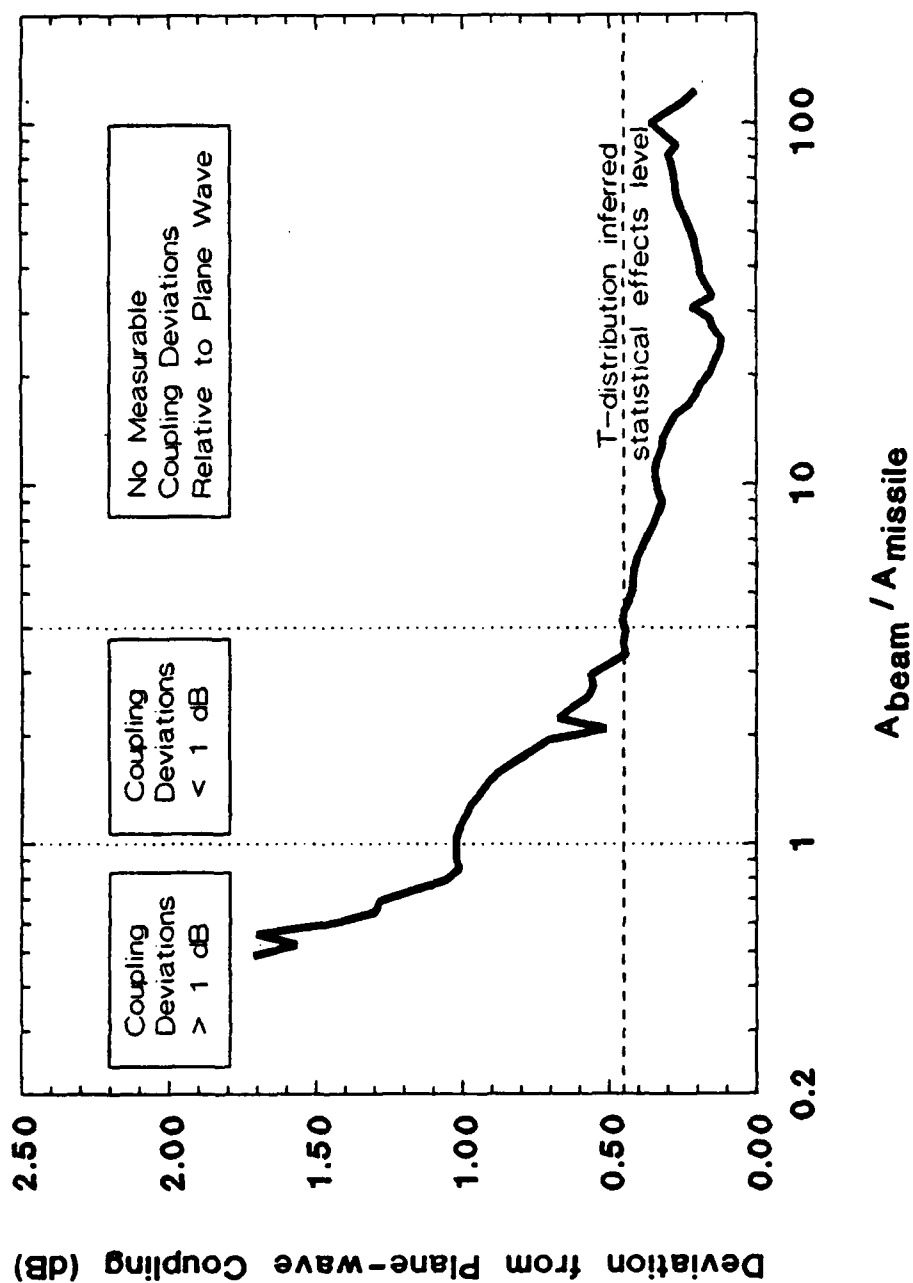


Figure 3. Deviation from plane-wave coupling conditions, measured as variations in  $A_{eff}$  of three in situ Maverick missile probes. The curve is an average of absolute deviations of  $A_{eff}$  at 36 frequency peaks in L- and S-bands (average of Fig. 2 data).

beam effective area are shown in Figure 4 for two representative frequencies.  $A_{\text{missile}}$  is defined as the missile window area (projected flat) since the window is assumed to be the main point-of-entry for head-on illumination. The data of Figures 2 and 3 clearly show that departure from plane-wave coupling conditions increases as  $A_{\text{beam}}/A_{\text{missile}}$  decreases, demonstrating the more general link between uniformity of illumination and plane-wave-like coupling conditions.

#### EFFECTS OF STANDING WAVES

There was no evidence of departure from plane-wave-like coupling due to standing waves between the horn and missile. Under conditions where unperturbed illumination of the missile is uniform to  $\pm 1.5$  dB (valid for all radiating near-field locations actually used in HPM testing of Maverick at WL), any waves reflected from the missile and subsequently reflected by the horn are not of sufficient amplitude to significantly affect coupling. Any slight differences in coupling may be attributed to the slightly nonuniform illumination. Experimental measurements of the reflected RF power were generally consistent with theoretical/empirical models utilizing the NEC-BSC code.

A comparison of measured and calculated reflected power relative to incident power is shown in Figure 5 for a missile to antenna output aperture distance of 41 cm. For calculation, the missile was modeled as a circular cylinder with a 2-in-dia disk located at the IR eye position just inside the IR window. The scattered radiation was computed using the geometric theory of diffraction (GTD) implemented in NEC-BSC. Reflected power from the missile back into the horn was generally 20 dB or more below the incident power, suggesting that the formation of standing waves (which required *multiple* reflections) is unlikely to cause meaningful departures from plane-wave coupling under test conditions ( $z > 41$  cm).

#### REACTIVE COUPLING EFFECTS

There was no experimental evidence of departure from plane-wave-like coupling due to reactive effects at any radiating near-field locations examined. This was expected, since reactive coupling decreases very rapidly with distance. In fact, computed reactive power densities (determined from the imaginary part

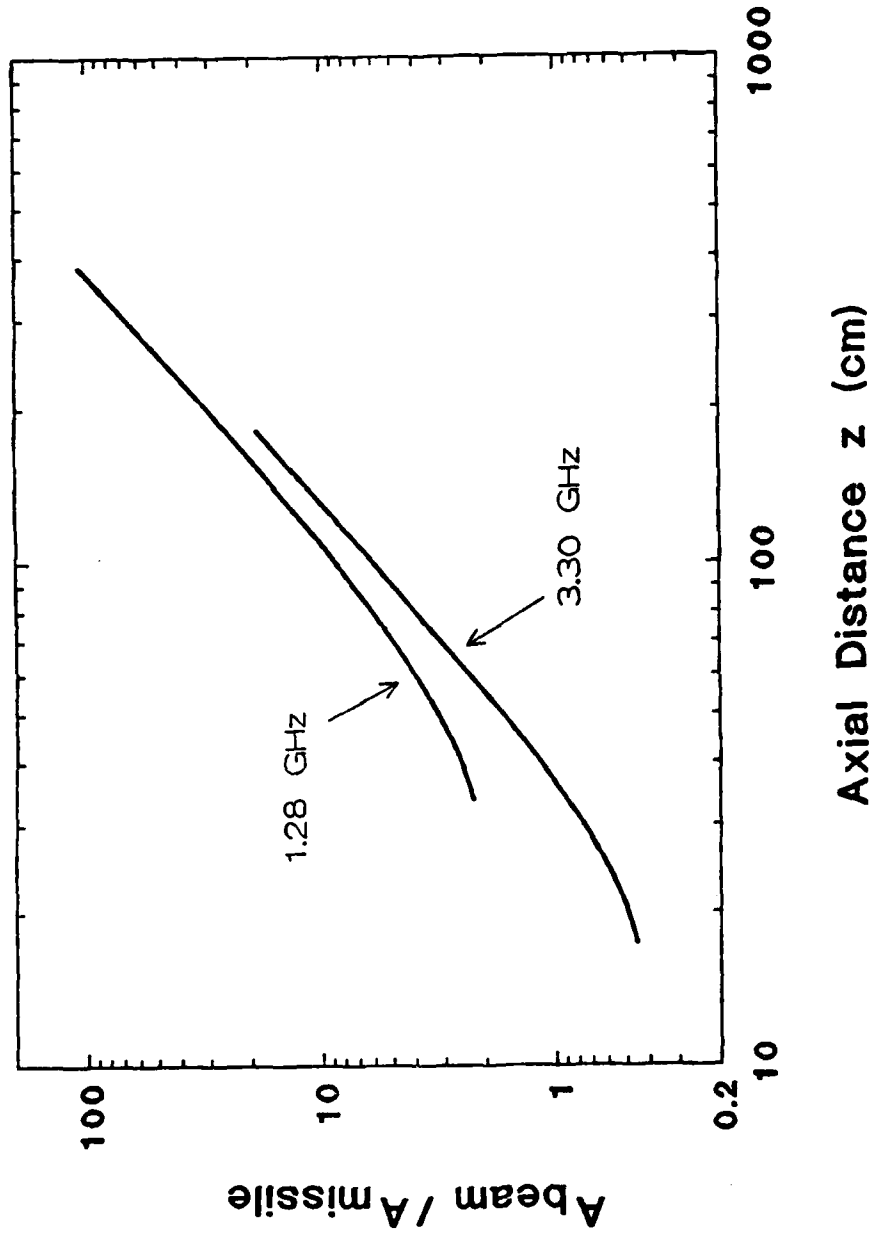


Figure 4. Calculated beam cross-sectional area versus axial positions z at two representative frequencies, for Narda L- and S-band standard gain horns.

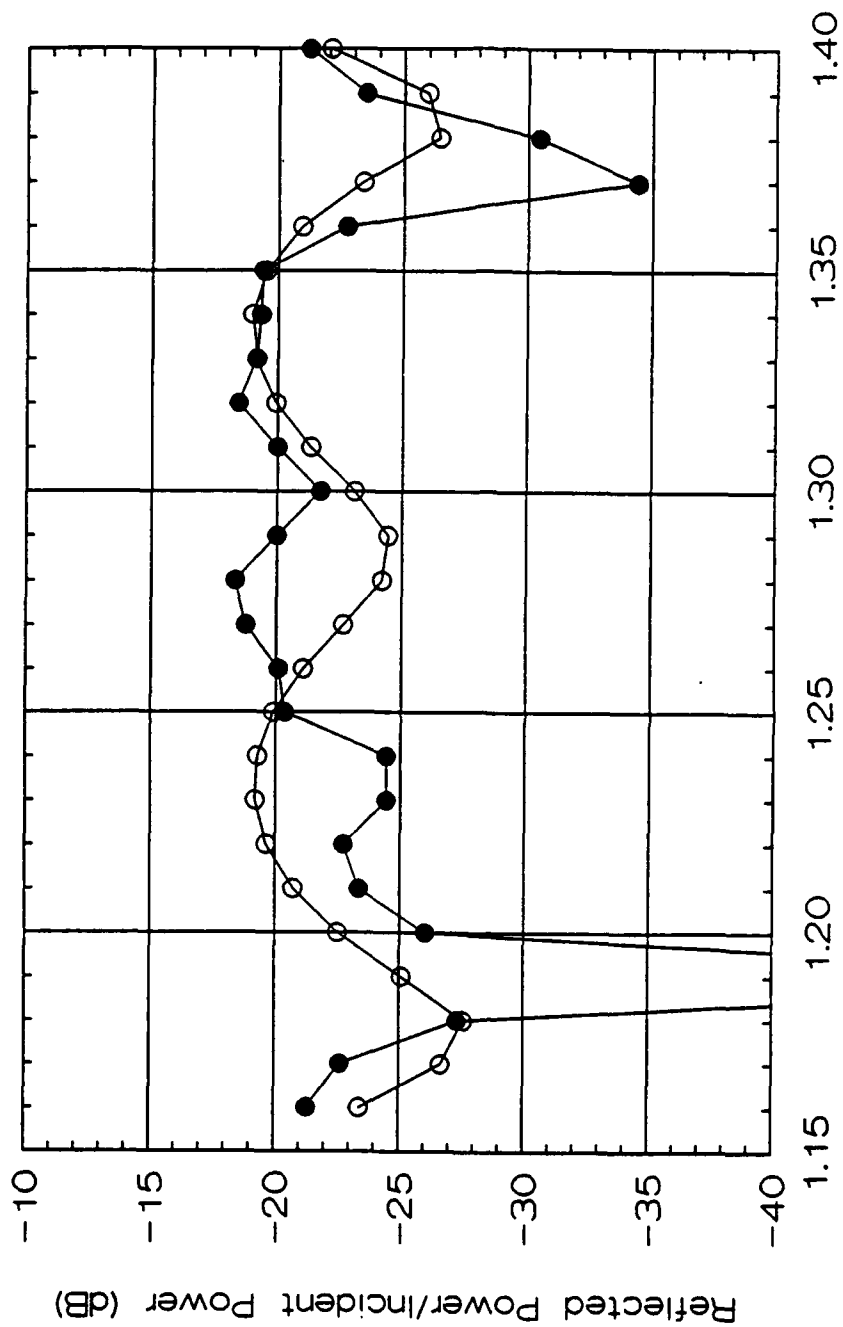


Figure 5. Reflected power/incident power as measured in L-Band (solid circles) and calculated with NEC-BSC GTD model (open circles) with missile 41 cm from the horn aperture.

of the Poynting vector, which tends rapidly to zero with increasing  $r$ ) were always 20 dB or more below radiated power densities. Placement of the missile at a distance exceeding two wavelengths from the aperture was more than sufficient to result in a completely negligible level of reactive coupling. For S-band, testing with the standard gain pyramidal horns utilized, simply requiring that uniformity of illumination be no worse than  $\pm 1$  dB over the window implied an aperture-to-missile separation exceeding two wavelengths anyway. For L-band, departure from plane-wave-like coupling was not found to be particularly significant even at separations of only one wavelength. Note that actual high power susceptibility testing will be performed only at distances exceeding two wavelengths, i.e., well beyond the reactive near field.

### CONCLUSION

This study will allow testing of the Maverick missile at unprecedented power levels and energy fluences with good confidence that the coupling conditions are equivalent to plane-wave illumination. The results suggested applying a simple empirical rule for the Maverick test:

If  $A_{\text{beam}}/A_{\text{missile}} \geq 2$ , then the relative coupling will be within  $\pm 1$  dB of plane-wave conditions.

For the WL horn antennas used to test the Maverick missile, this rule is much less restrictive than needlessly insisting that the missile be placed at  $> 2 D^2/\lambda$  from the aperture. As a result, depending on the particular frequency and horn geometry, the Maverick missile can be tested at power densities and energy fluences up to 10 dB greater than those available at  $r \geq 2 D^2/\lambda$ . This general relation between uniformity of illumination and departure from plane-wave coupling conditions is useful in evaluating the validity of test configurations involving broader classes of antennas and test objects.

REFERENCES

1. Microwave Scanning Antennas, ed. by R. C. Hansen, "Apertures," Vol. 1, p. 36, 1985.
2. Johnson, R. C. and Jasik, H., Antenna Engineering Handbook, Chapter 1, McGraw-Hill, New York, 1984.
3. Koslover, R. A., Cremer, C. D., Geren, W. P., Voss, D. E., and Miner, L. M., "A Compact High-Power Broadband  $TM_{01}$  to  $TE_{11}$  Circular Waveguide Mode Converter," Bull. Am. Phys. Soc., Vol. 34, No. 9, p. 2073, October 1989.

## APPENDIX

## ANTENNA CODES

This appendix describes the radiating near-field/far-field code used in the data reduction for this work. Based on a number of cross-comparisons with other work, both experimental and theoretical, the power densities calculated are accurate to  $\pm 0.2$  dB.

COMPUTATION OF THE RADIATING NEAR FIELDS

With detailed knowledge of the E and H fields over a closed surface enclosing all the source(s), the external radiated fields (in the reactive, radiating near-field and far-field regions) may be computed exactly (Ref. A-1). However, such complete information is virtually never available. Instead, it is customary to consider only the aperture fields of the antenna. Fields elsewhere are assumed negligible for the purpose of computing the radiated field. Aperture fields are estimated by extrapolation of the driving waveguide fields, including a correction for phase error (nonuniformity of phase across the aperture). This technique is applicable to flared horn antennas, but it is less useful for small apertures such as open-ended waveguide (Ref. A-2) due to neglect of diffractive effects.

In computing patterns from conical and pyramidal horns typically used in HPM effects testing, it is generally valid to ignore edge diffraction. The aperture integration method used is the Stratton-Chu approximation (Refs. A-1 and A-3). Like other aperture integration methods, the Stratton-Chu method loses accuracy for large polar angles, and it is useless in the computation of backlobes. These regions are of little interest in HPM effects testing.

The formulation is essentially the same as that used by Li and Turrin to compute radiated near-field patterns from  $TE_{11}$ -driven conical horns, although we keep one additional small term that Li and Turrin dropped. The expression for the radiated electric field,  $E_p$ , is:

$$\mathbf{E}_p = - \frac{jk}{4\pi} \int_{\text{Aperture Surface}} \hat{\mathbf{R}} \times \left[ \hat{\mathbf{n}} \times \mathbf{E}_a - \eta \hat{\mathbf{R}} \times \left( \hat{\mathbf{n}} \times \mathbf{H}_a \right) \right] e^{(-jkR)} / R \, dS \quad (\text{A-1})$$

In Equation 1,  $\eta = (\mu_0/\epsilon_0)^{1/2} \approx 120\pi$  (impedence of free space),  $\mathbf{E}_a$  and  $\mathbf{H}_a$  are the aperture fields, which depend on the driving waveguide mode and the horn geometry,  $\hat{\mathbf{n}}$  is the unit outward normal to the aperture surface,  $R$  is the magnitude of the vector pointing from the integration point on the aperture to the fixed measurement point, and  $\hat{\mathbf{R}}$  is a unit vector along this direction. Equation A-1 may be applied to an aperture of arbitrary shape. The radiated magnetic field,  $\mathbf{H}_p$ , is computed separately by replacing the integrand in the previous expression (denoted by  $d\mathbf{E}_p$ ) by  $d\mathbf{H}_p$  which is given by:

$$d\mathbf{H}_p = \hat{\mathbf{R}} \times d\mathbf{E}_p / \eta \quad (\text{A-2})$$

and then integrating as before. Thus, the complex  $\mathbf{E}_p$  and  $\mathbf{H}_p$  fields may be computed in the radiating near-field region.

#### RADIATING NEAR-FIELD CODE VALIDATION

Radiating near-field patterns computed by numerical integration using Equations A-1 and A-2 were validated both experimentally and theoretically in a variety of ways. For the TE<sub>11</sub>-driven conical horn, we may compare directly the results to E- and H-plane patterns computed (and verified experimentally) in Reference A-4. The agreement is excellent, typically  $\pm 0.2$  dB as shown in Figure A-1. The conical and pyramidal horn computations were also compared to the results obtained from aperture integration using the NEC-BSC code (Ref. A-5). An example comparing the on-axis power density radiated by a Narda standard gain horn as computed by the two codes is shown in Figure A-2. Again, the agreement is excellent, typically  $\pm 0.2$  dB. Finally, free-field diagnostic measurements performed to characterize HPM sources and antennas at WL have also shown excellent agreement with computed conical and pyramidal horn antenna patterns.

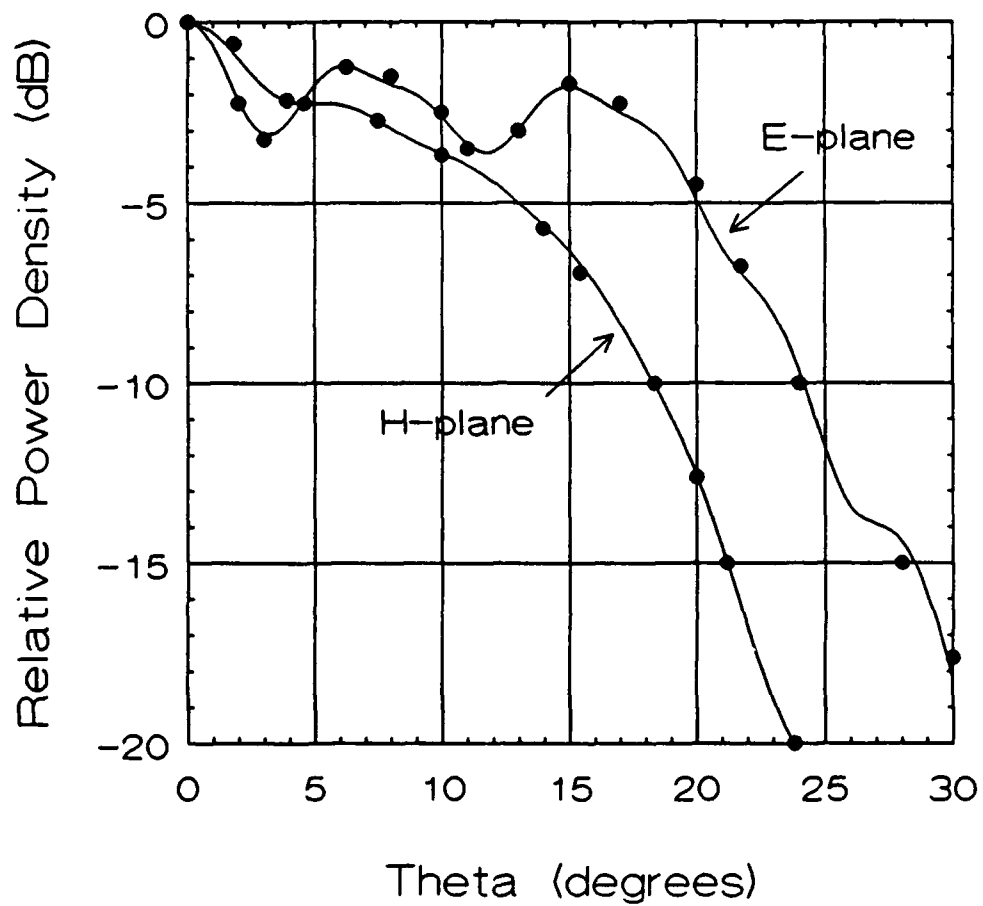


Figure A-1.  $TE_{11}$  code predictions (lines) and results found by Li and Turrin (dots) for an x-band horn at  $r \approx 0.1 D^2/\lambda$ .

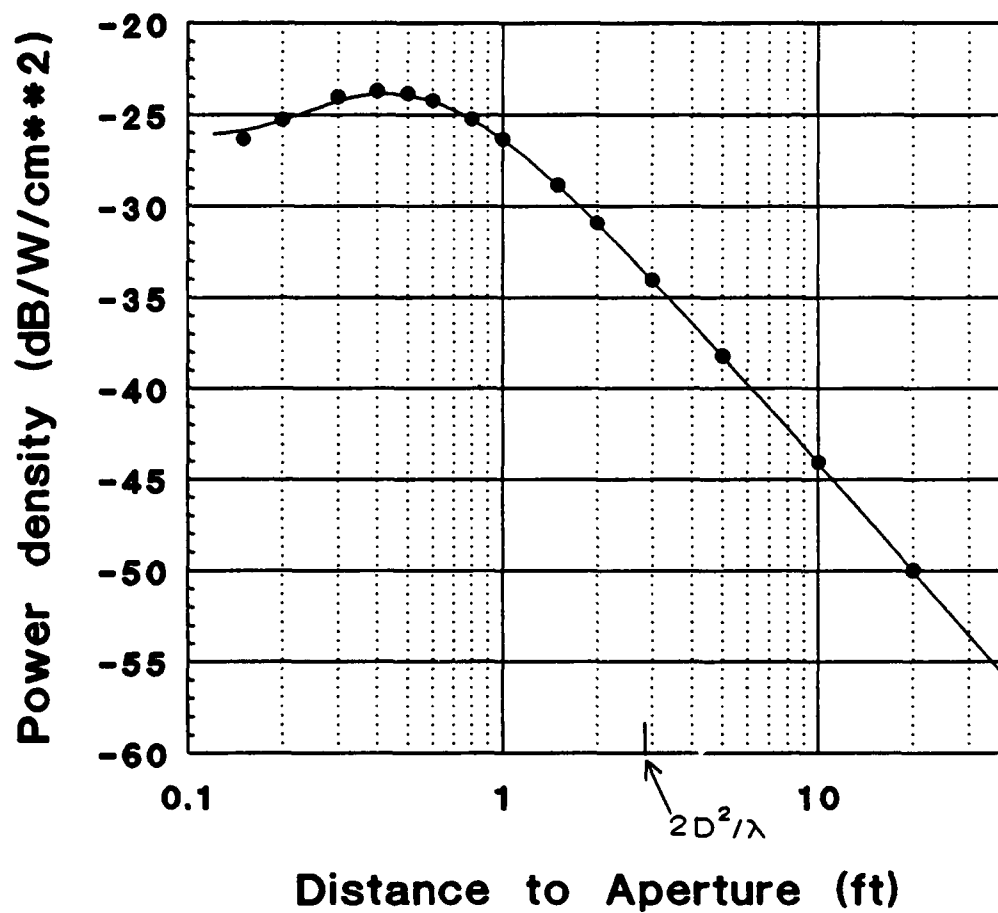


Figure A-2. Comparison of present TE<sub>10</sub> code (line) to NEC-BSC code (dots) for a Narda 644 standard gain horn at 3.3 GHz and 1 W.

FAR-FIELD CODE VALIDATION

The calculated and measured far-field gain was compared to that provided by Narda for their WR-284 standard gain horn. Excellent agreement was found across the entire band, typically  $\pm 0.2$  dB or better, as shown in Figure A-3. Narda's gain curves are based on antenna-range experiments and are claimed accurate to  $\pm 0.3$  dB by the manufacturer.

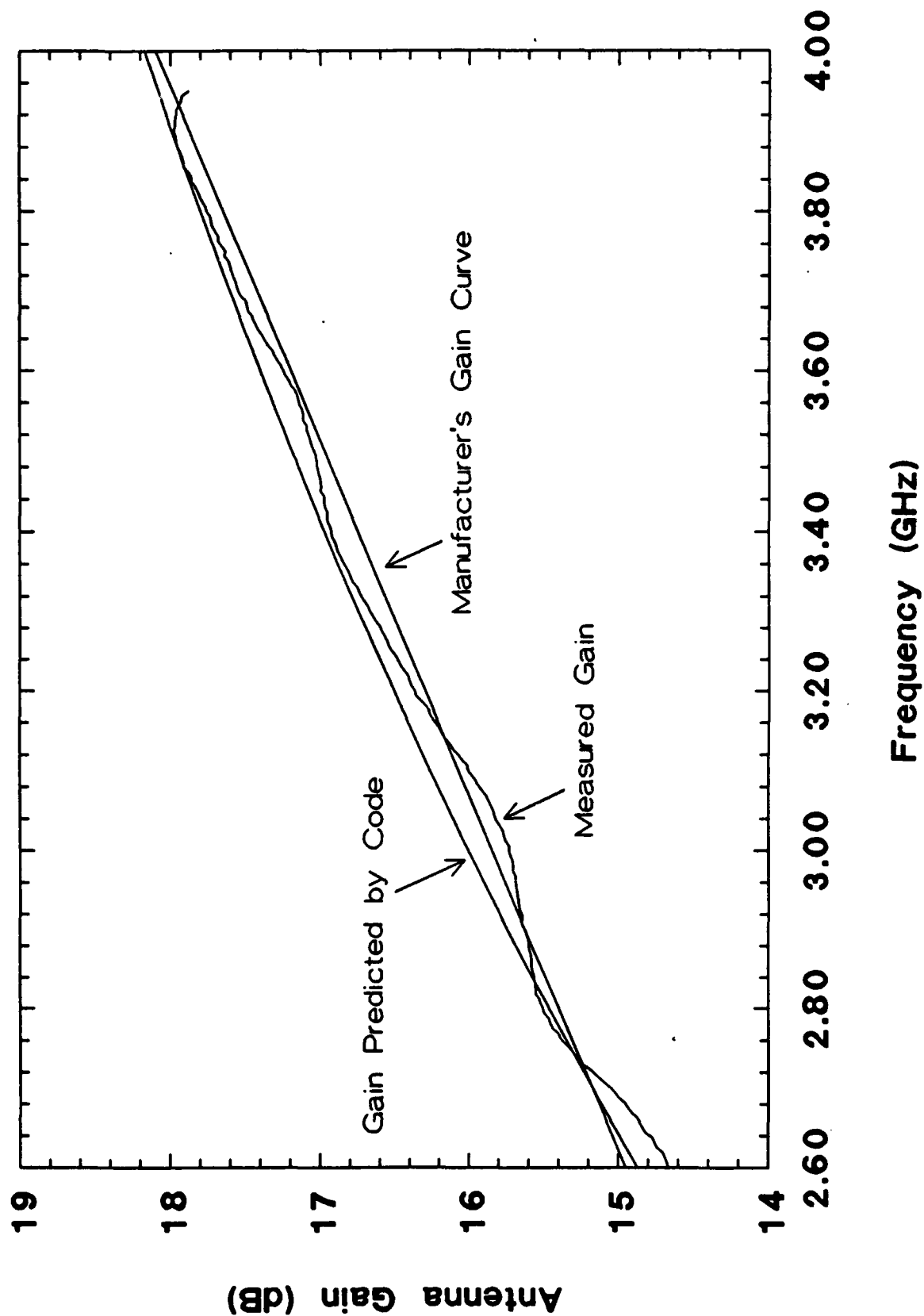


Figure A-3. Comparison of calculated gain, measured gain and manufacturer's provided curve.

REFERENCES

- A-1. Silver S., Microwave Antenna Theory and Design, M.I.T. Radiation Laboratory Series, Vol. 12, McGraw-Hill, New York, 1949.
- A-2. Cremer, C. D.; Voss, D. E.; Koslover, R. A.; and Silvestro, J., "Effective Area of Unflanged Open-Ended Rectangular Waveguide Used as a Free-Field Sensor," Proceedings of the Narrowband (HPM) and Wideband RF Propagation/Phenomenology/Methodology Workshop, Lawrence Livermore National Laboratory, California, October 23-26, 1989; to be presented at the Fifth National Conference on High Power Microwave Technology, West Point, New York, 10-15 June 1990.
- A-3. Stratton, J. A., Electromagnetic Theory, McGraw-Hill, New York, 1941.
- A-4. Li, T., and Turrin, R. H., "Near-Zone Field of the Conical Horn," IEEE Trans. Ant. & Prop., pp. 800-803, Nov. 1964.
- A-5. Numerical Electromagnetic Code - Basic Scattering Code. User's Manual, Ohio State University, 1982.